

University of Gothenburg

M.Sc Thesis

On-line quantification of ^{211}At at distillation

Author: Susanna Crafoord-Larsen

Supervisor: Sture Lindegren



Department of Radiation Physics

2010

Table of contents

Abstract.....	3
Introduction.....	4
Material and methods.....	6
General	6
Technical facts	7
System Setup	8
Astatine-211 (²¹¹At).....	11
Technetium-99m (^{99m}Tc).....	14
Results.....	16
Discussion.....	32
Conclusion	34
References	36
Acknowledgements	37

Abstract

The use of ^{211}At as a tumor-targeted radiotherapy is a relatively new process. At the Sahlgrenska University Hospital the technique have been investigated for the last 15 years. At the time of this thesis the research has lead up to a phase I study with with nine subjects with the aspiration of implementing the technique on three additional patients this year. At the Sahlgrenska University Hospital the research has been concentrated around the treatment of micro metastases that originates from ovarian cancer.

In this work a NaI detector system is set up to measure the build-up graph of the distillation process, to calculate an activity calibration factor that converts the CPS registered in the NaI to activity and also conduct measurements to verify or disprove the presence of any contaminations of in the process.

Introduction

The alpha(α)-particle emitter ^{211}At has drawn attention as a good candidate for targeted alpha therapy, e.g. radio immunotherapy. This is due to the fact that it is an alpha-particle emitter and also because of its chemical characteristics. At the current state micro metastases can be difficult to treat with traditional methods using electron emitters. ^{211}At decays in two branches with a half-life of 7.2 h into the stable ^{207}Pb (kanske en fig).

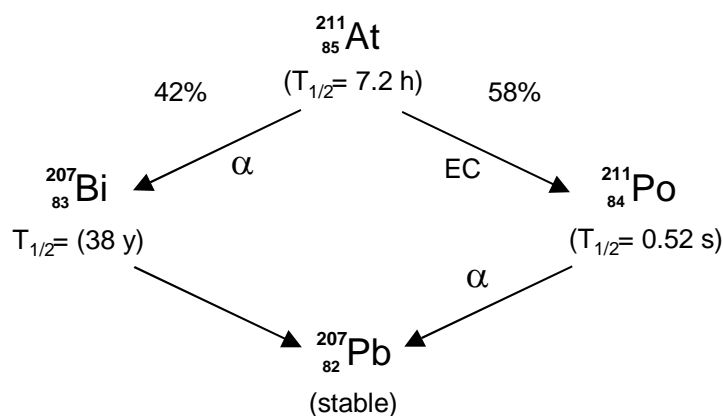


Figure 1: The decay scheme of ^{211}At into ^{207}Pb

The alpha particles emitted have a mean energy of 6.5 MeV and for human tissue this correlates to a distance $\sim 65\mu\text{m}$ (a typical cell size is around $10\mu\text{m}$). Research in the field of α -particle emitting radio immunotherapy seems to be an important complement to external radiation therapy, surgery and intravenous combination chemotherapy.

Even though pathologically complete remission is obtained with intravenous combination chemotherapy; up to 50% of afflicted patients will suffer from tumor regrowth due to undetected micro metastases. Intraperitoneal administration with ^{211}At bound to specific monoclonal antibody is an attractive treatment because the antibody binds specifically to the target tumor and brings the radionuclide close to the tumour cells. This not only

eases the treatment of micro metastases but also minimizes the stress to unaffected, healthy tissue. The preclinical work has resulted in a phase I study (i.e. the first stage of testing in human subjects) of the treatment of the ovarian carcinomas at Sahlgrenska University Hospital, Gothenburg, Sweden (Andersson H, et al, 2009). The aim of this thesis has been to evaluate, calibrate and optimize a detector setup for on-line measurement ²¹¹At in the distillation process, in such that information about activity in the different stages can be retrieved, if there are any contaminations and get a first look at the build-up graphs.

Material and methods

General

The astatine was delivered in form of a target, an aluminum backing of approximately 30 X 28 X 5 mm with a thin layer of bismuth with a thin layer of aluminum added on top. The Bi layer was in the range 18-20 mg/cm² and the additional layer of Al was around 2 mg/cm² (Lindegren et al 2007). The targets were built and prepared at Chalmers University, Gothenburg, Sweden and shipped to Rigshospitalet in Copenhagen, Denmark, where the cyclotron was located. The target was bombarded with 26 MeV alpha particles to create ²¹¹At in the bismuth layer by ²⁰⁹Bi(α , 2n)²¹¹At. The backing and coating functioned as a cooling system during the irradiation and as a confinement for the bismuth because of its fragile nature. The target can be seen in figure 1, below.



Figure 2: *The target as it were after the ²¹¹At was removed.*

Detectors: Technical facts

The in house ionization chamber in the laboratory: CRC-15 dose calibrator ionization chamber produced by Capintec, IA, USA.

The Sodium Iodide detector used: Sodium Iodide (TI doped) well crystal detector. Scintillation crystal, Serial BO-247, Type 7SF8/2A, Harshaw Chemie BV, Holland. Electronics, MOD P-14, S/N AD-547, Bicron Corp, USA.

The ratemeter (see figure X) used with the Sodium Iodide detector: ESM/FAG Ratemeter FHT 1100, Z-Nr 42495/01, F-Nr 00914, ESM Eberline, Erlangen Germany

The High Purity Germanium (HPGe) detector used: Ortec GMX-10200 series HPGe GAMMA-X - HPGe-High Purity Germanium Coaxial Photon Detector system (Serial No. 22-N862C)

The Multi Channel Analyzer connected to the HPGe detector: Ortec MCA device (DSPEC jr.2-Digital Gamma-Ray Spectrometer) sr. 07128442.

On-line Detector System Setup

In order to be able to monitor the distillation process of ^{211}At a new detector setup was evaluated and calibrated. The system prior to this project was a NaI detector with an analog display. This previous system gave the observer no information about the activities involved in the different processes or the appearance of the build-up curve in the distillation process (described later). A NaI detector was the detector of choice for the daily routine, mainly because of the simplicity of the system. Although limited in technicalities it needed not to be more advanced at the current state. But a rate meter with some desirable properties was introduced as a replacement to the system used previously. Also, the NaI-detector was replaced with a well crystal detector instead of the previous planar detector, which was attached to the analog count reader. The NaI detector was collimated with a custom built lead tube of 30 cm in length. This was important because the laboratory in which the distillation, and therefore also the measurements, took place contained a number of other radionuclides. The detector rests on a custom made stand and a Styrofoam holder, that was measured and cut and altered for optimal measurement angle and height, holds up the collimator. For detector aiming purposes a laser pointer was attached on the detector using tape and the detector was aimed using eye measurement. The NaI-detector system was tested with $^{99\text{m}}\text{Tc}$ to see if it was stable and fully functioning since it had not been used for some time. The use of $^{99\text{m}}\text{Tc}$ instead of ^{211}At was due to the fact that ^{211}At is only delivered to Sahlgrenska University hospital every other Wednesday and a molybdenum generator is always present at the department of nuclear medicine. The NaI-detector setup with collimation and holders can be seen in Figure 1. The rate meter used together with the detector was set to counts per second (CPS) and the energy window in which the measurements were carried out was kept almost open, i.e. almost the whole spectrum was measured. The astatine x-ray peak cluster (ranges from energies $\sim 78\text{-}90$ keV) was unfortunately cut a bit when the NaI system was first energy calibrated.



Figure 3: *The NaI detector with the lead collimation and Styrofoam support. The detector was positioned on a bench approximately two meters from the measuring point.*

Since the energy resolution of a NaI detector is relatively low, a HPGe detector was introduced for cross calibration. The goal with this was to identify contamination of any sort that may originate from the production of ^{211}At . The HPGe detector was energy calibrated with calibration samples of low activity. The electronics, earlier described, did not provide an on-line quantification but instead required a manual reading after the measurement. However, it did provide a numerical value of measurement.

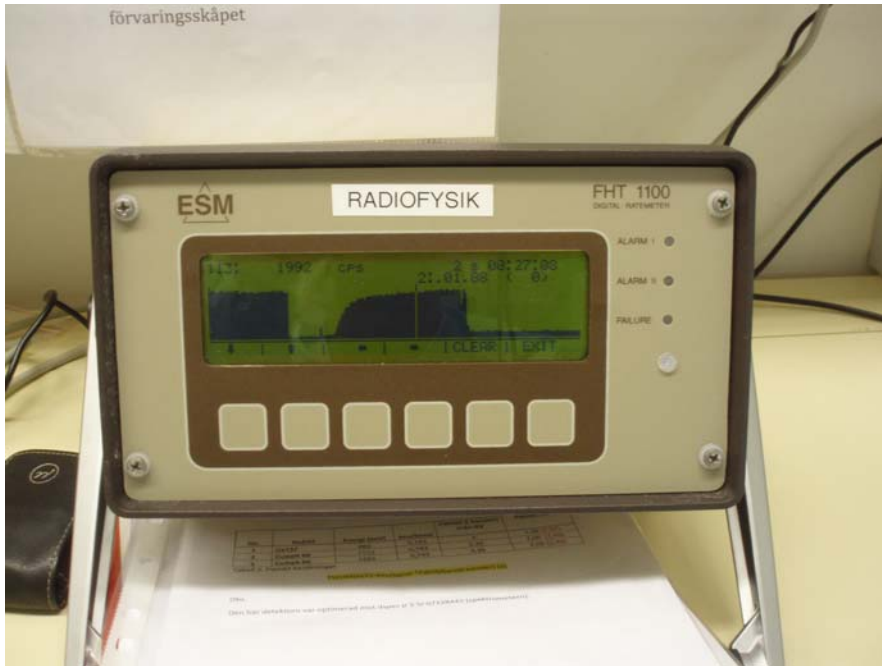


Figure 4: *The ESM rate meter.*

The CPS histogram (retrieved from the ratemeter) can be seen in Figure 2. The channels were read out manually and the graphs were plotted in excel. These can be viewed in Results.

Measurements included the intact target straight from delivery, the scraped target, the scrapings and during the distillation process. In order to ensure correct measurements, background measurements were completed prior every measuring session. Also, background measurements were conducted before every session because the setup was placed in a laboratory used for a variety of different nuclides and experiments. See Figure 3 below for an image of the measurement of the scrapings.



Figure 5: *The scrapings in the quartz boat. To be able to balance the boat, it was placed on bunched up paper. An empty PEEK tube (used in the distillation process) is noticeable in behind the boat.*

Measurement of Astatine-211 (^{211}At)

The ^{211}At measurements were conducted every other Wednesday when the ^{211}At was delivered to the Sahlgrenska University Hospital and were divided into different steps. The target was measured upon delivery both in the stationary ionization chamber (IC) and placed in the Styrofoam cylinder and measured with the NaI-detector system. The irradiated target material was removed by scraping the Bi-Al layer from the backing, resulting in small flakes of Bi-Al. The activity of the scrapings was calculated by subtracting the remaining activity in the backing from the total activity of the target. The scrapings were not measured in the IC due to practical reasons, i.e. the scrapings could have been spread around the room or in the IC thus contaminating it. The NaI detector measured the scrapings for the activity

calibration. The scrapings were contained in a quartz boat (a cylinder made of quartz) due to its heat resisting properties.

The procedure was done in this fashion because of the risk of contaminating the IC and of spreading the scrapings in the room and thus not only contaminating the room but also losing ^{211}At . On one occasion an activity measurement of the scrapings in the IC was conducted as an assurance that the usual way of performing the activity measurement was not too off. After this the quartz boat was placed in the oven and the scrapings were heated to about 670°C . On the other end of the oven a polyetheretherketon (PEEK) tube was connected that leads down to a loop in a Styrofoam cylinder that was filled with a mixture of dry ice and ethanol that worked as a cryo trap, condensing the ^{211}At in the tube, i.e. trapping it (see Figure 4 below).



Figure 6: *The PEEK tube from the oven (through the hole to the right) leading down into the Styrofoam cylinder.*

The PEEK tube was connected to an E-spot which was joined with a gas wash bottle followed by an additional E-spot that was connected to a tap water jet pump creating reduced pressure within the system. The gas wash bottle contained a reducing agent, which functioned as a safety measure trapping

any un-condensed ^{211}At . The two E-spot flasks were guarding the system from liquid being flushed back into to the hot oven.

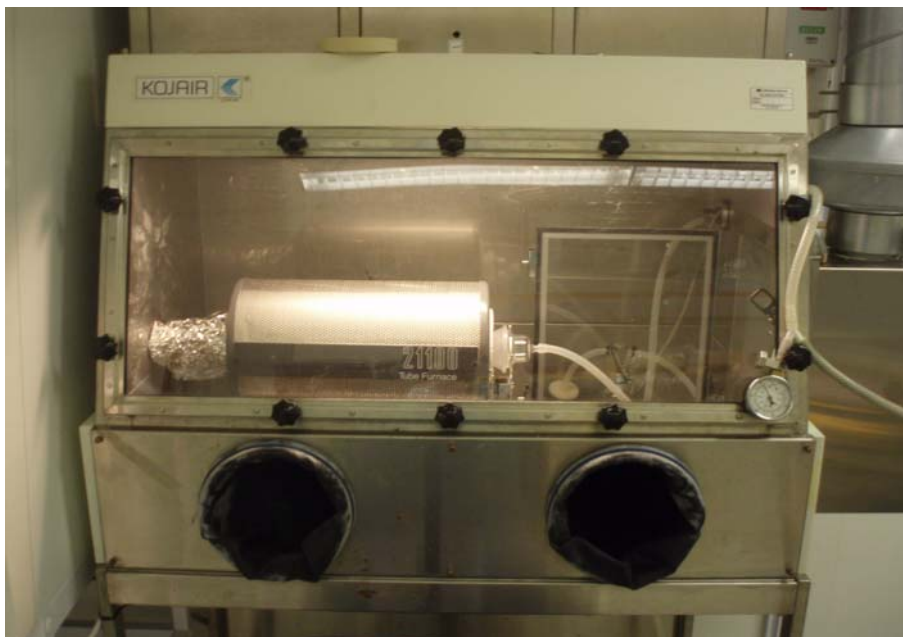


Figure 7: *The glass cage with the oven used for distillation of ^{211}At . The tubing and pressure gate to the right belongs to the nitrogen supply system.*

The water jet pump on the outlet side created, with the help of running water, reduced pressure throughout the entire system to get the vaporized ^{211}At to flow in the wanted direction, i.e. into the cryo trap. This setup can be seen in Figure 6 below. The low pressure throughout the setup also prevented any ^{211}At from leaking out from the oven and contaminating glove box , where the oven is located (see Figure 5), or even contaminating the room and personnel. The pressure gradient was controlled by a counter flow of nitrogen gas connected to the inlet side of the oven, which prevents backflow. During all distillation occasion's measurements were performed and distillation-buildup curves were recorded. The results and analysis of these measurements can be seen in plot 1-5 and in Tables 8-10 in Results.



Figure 8: *The Styrofoam cylinder filled with dry ice + ethanol and the back flush safety system consisting of empty E-spots and a measuring glass filled with a binding agent.*

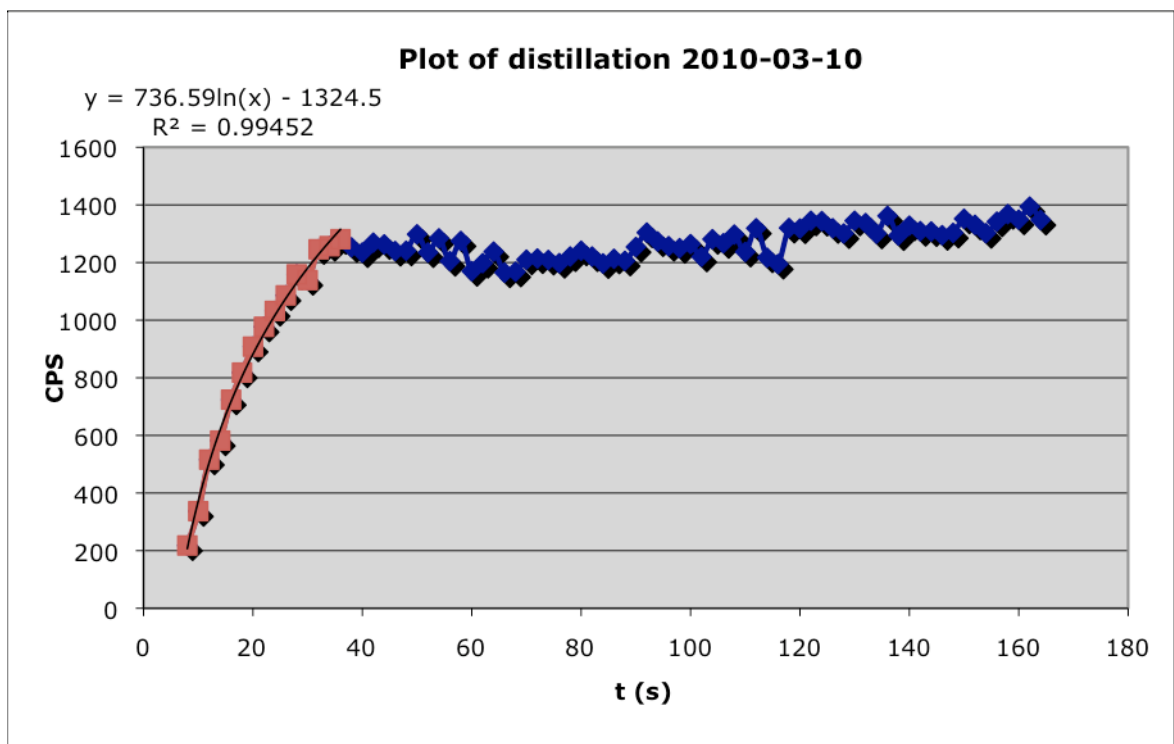
Technetium-99m (^{99m}Tc)

Because of the infrequency of the ^{211}At deliveries, ^{99m}Tc in the form of pertechnetate was used instead of the ^{211}At to imitate setup. The nuclide ^{99m}Tc was chosen because of the similarities with astatine with regards to energy and half-life. The distillation process geometry could not be imitated entirely but a tube with a stationary geometry was used to mimic this process. These measurements were performed to test the setup but also to try to calibrate it in terms of geometry and for activity measuring purposes. The simulated “target measurement” was a small volume of undiluted pertechnetate (in the range of $\sim 0.1\text{--}0.2$ mL). The results can be seen in Tables 3-4. The ionizing chamber, in the laboratory, which was used for all the activity measurements,

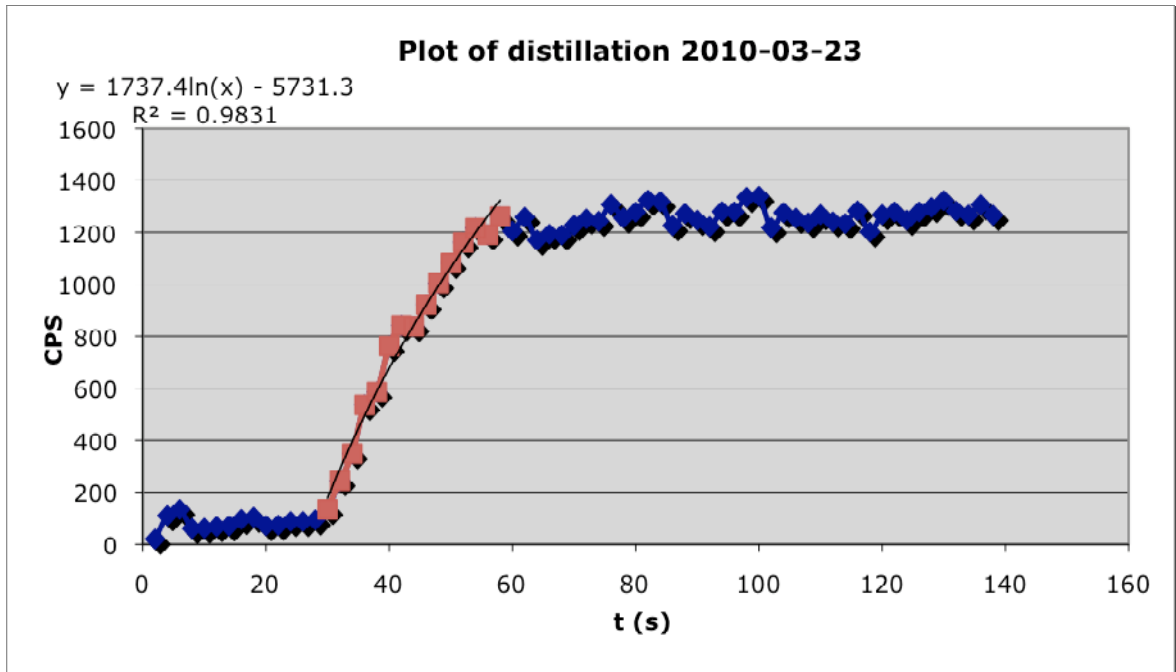
was calibrated for a volume of 10 mL of a liquid in a scintillation glass. To meet and to test the importance in keeping this geometry, a small volume of pertechnetate was diluted with phosphate buffered saline (PBS) to the volume of interest. Measurements with the IC and the NaI-detector in the ^{211}At geometry were performed and the results can be seen in Tables 1-2. The “stationary measurement” to simulate the geometry of the tubing during distillation consisted of a Teflon tube (at approximately the same length as the PEEK tube) filled with the simulated target from the “target measurement” diluted with PBS. Results of the measurements can be seen in Tables 3-4. A test in positioning was also conducted. A solution of pertechnetate and PBS (a total volume of 10mL) was elevated and lowered above the fume hood and the CPS at the different heights were measured and compared to the CPS results at the height of the Styrofoam cylinder. The Styrofoam cylinder height was assumed to be the height of maximum efficiency for the detector because the setup was (as mentioned earlier) calibrated to this position. The results for this measurement are shown in Table 5.

Results

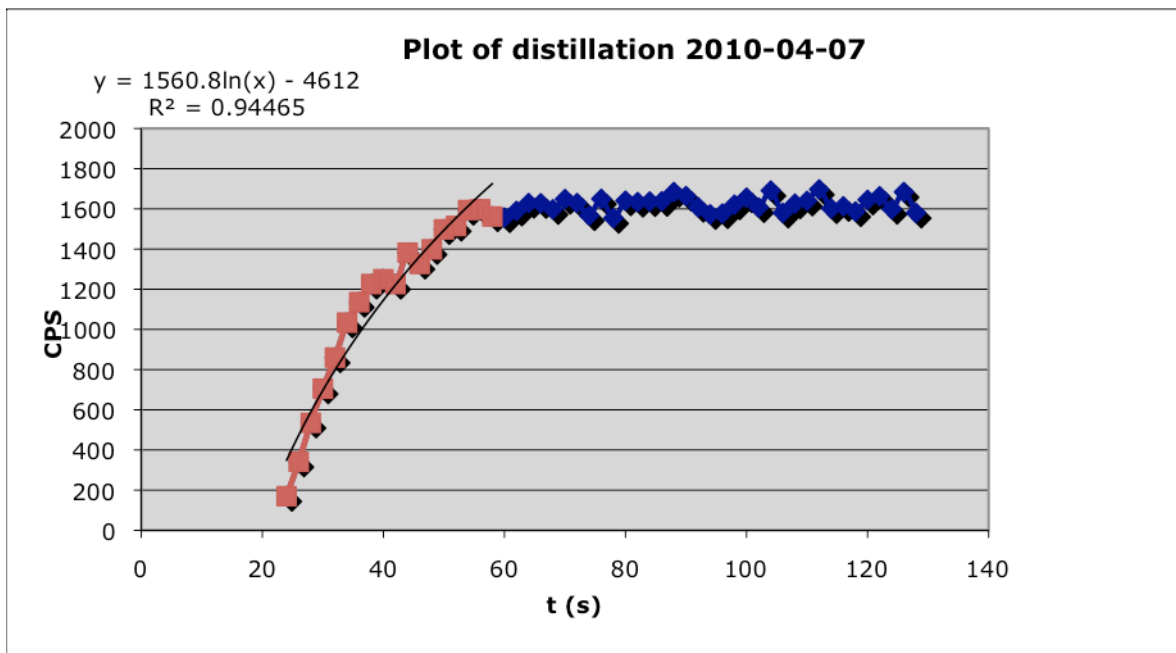
In Plots 1-5 the buildup curves of the distillation process are shown. For the distillation graphs, a trend line for the build-up part is included as a measurement of how equal each process is to the next. The running water (creating the low pressure) is turned down (thus decreasing the under-pressure) at around 90 s each measurement but the measurement continues past this. Each plot is a measurement at separate dates.



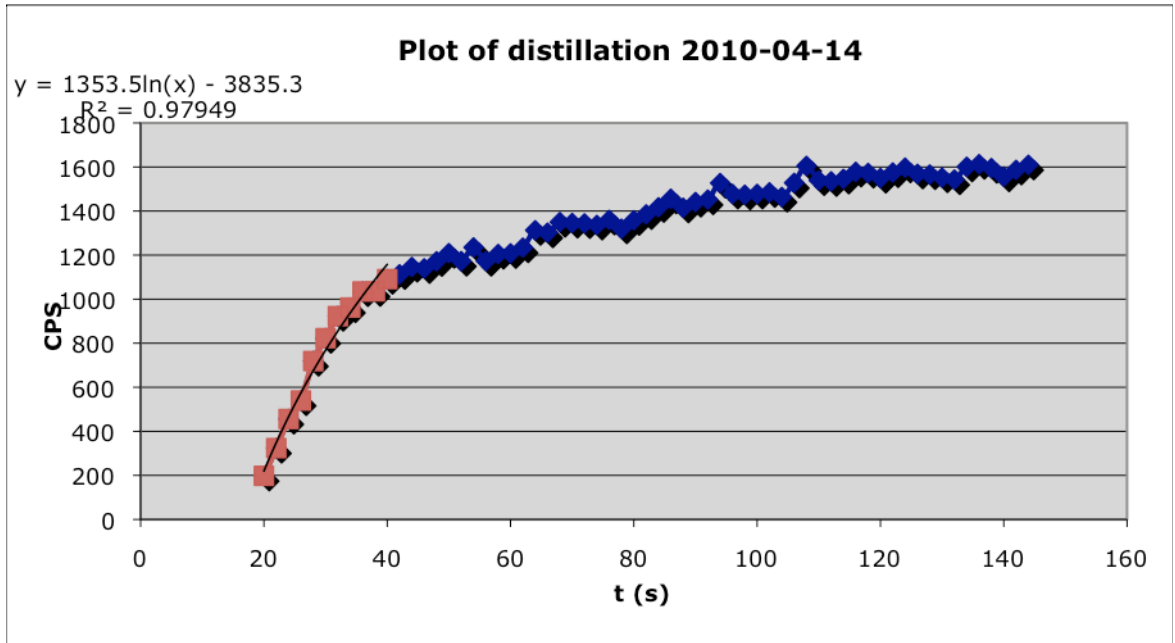
Plot 1: Distillation plot for measurement 2010-03-10. A trend line for the rapidly growing first part of the process is included.



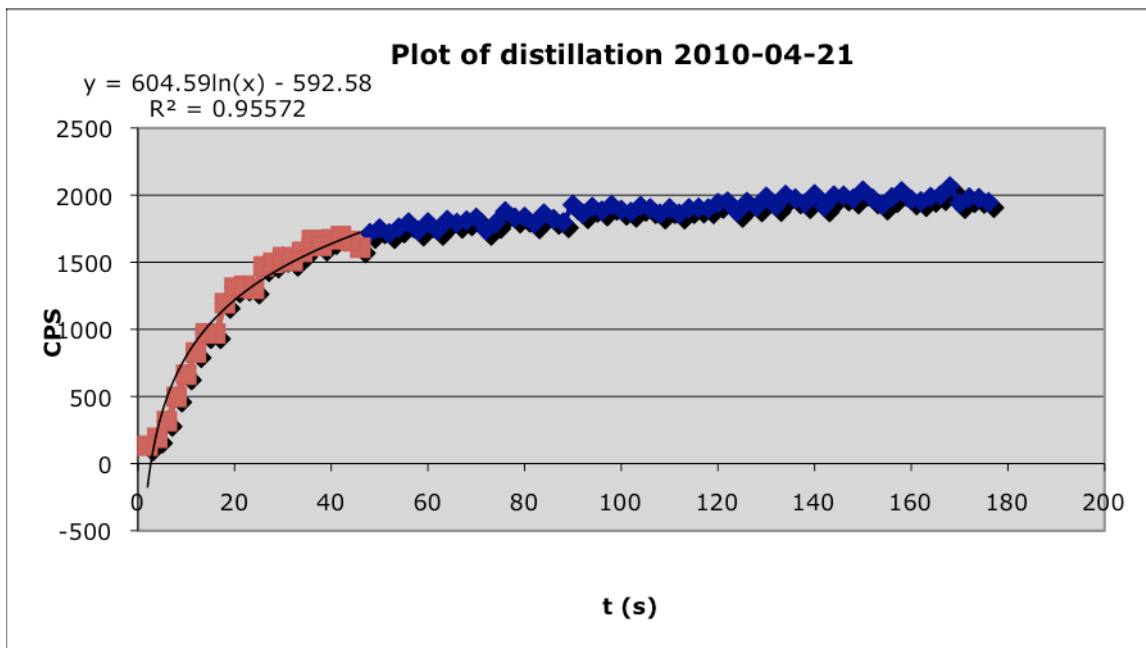
Plot 2: Distillation plot for measurement 2010-03-23. A trend line for the rapidly growing first part of the process is included.



Plot 3: Distillation plot for measurement 2010-04-07. A trend line for the rapidly growing first part of the process is included.

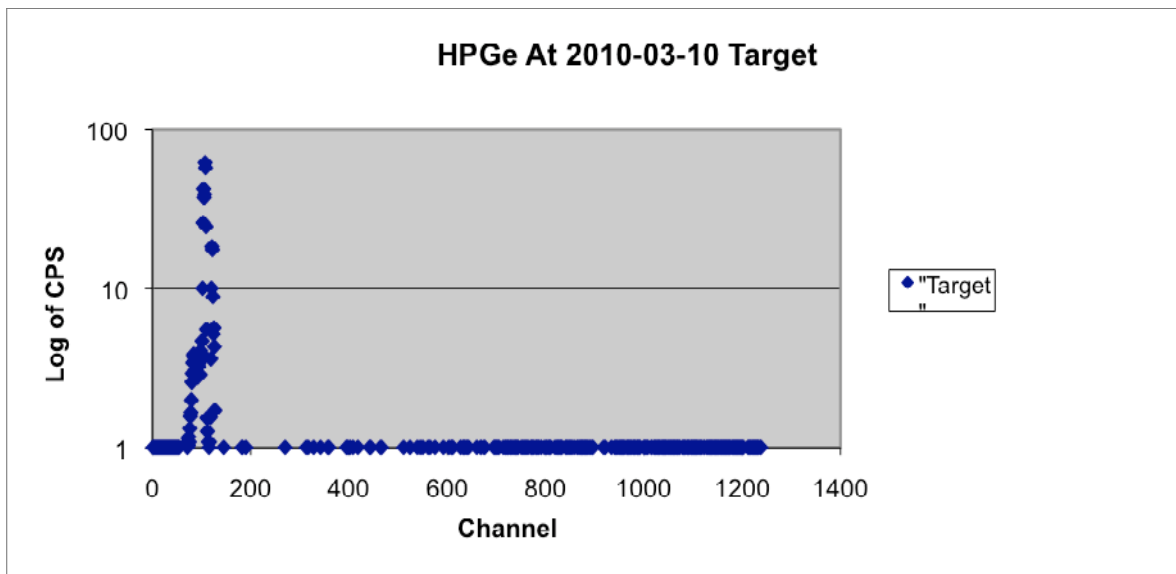


Plot 4: Distillation plot for measurement 2010-04-14. A trend line for the rapidly growing first part of the process is included.

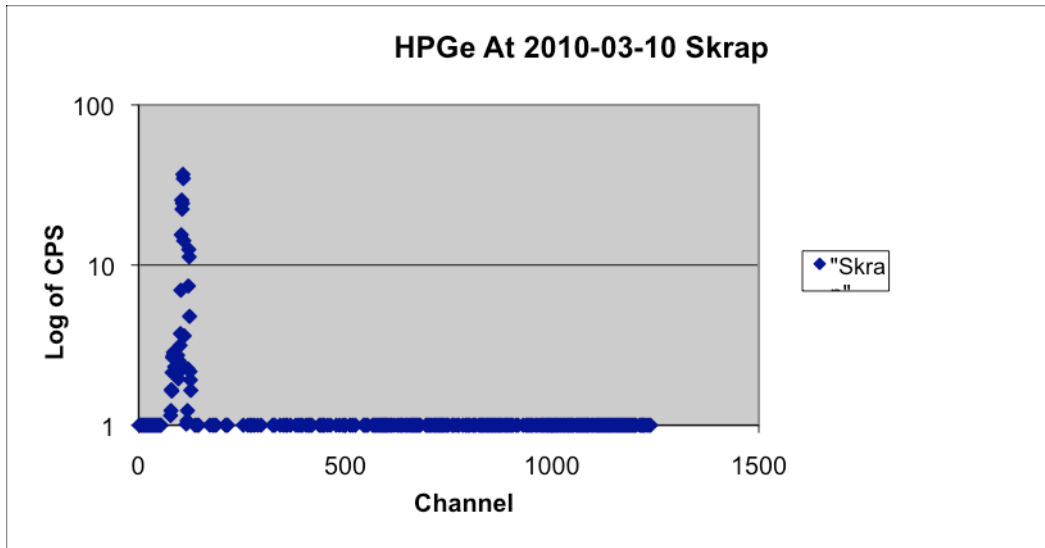


Plot 5: Distillation plot for measurement 2010-04-21. A trend line for the rapidly growing first part of the process is included.

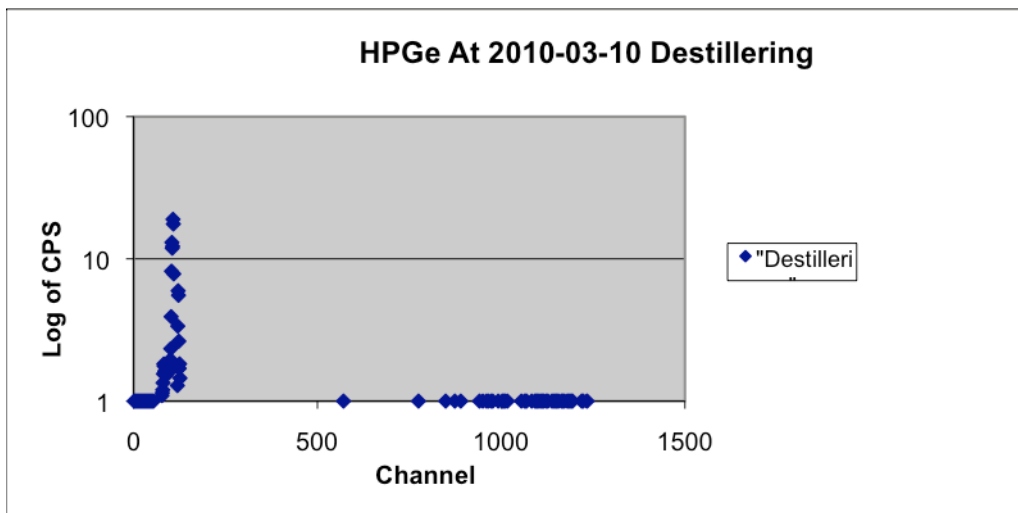
In Plots 6-11 below astatine measurements with the HPGe detector is shown. The HPGe was introduced to make sure that there were no contaminations in the target, and if there were any that they might continue along the process. As mentioned above the astatine measurements are divided into three subgroups. There are three different measurements (target, scrapings and distillation measurements) from two different dates. The scale is logged and the x-axis shows the channel number corresponding to a certain energy. To attain the energy the channel number was multiplied with the conversion factor, which was 0.743. This conversion factor was calculated when the detector was energy calibrated.



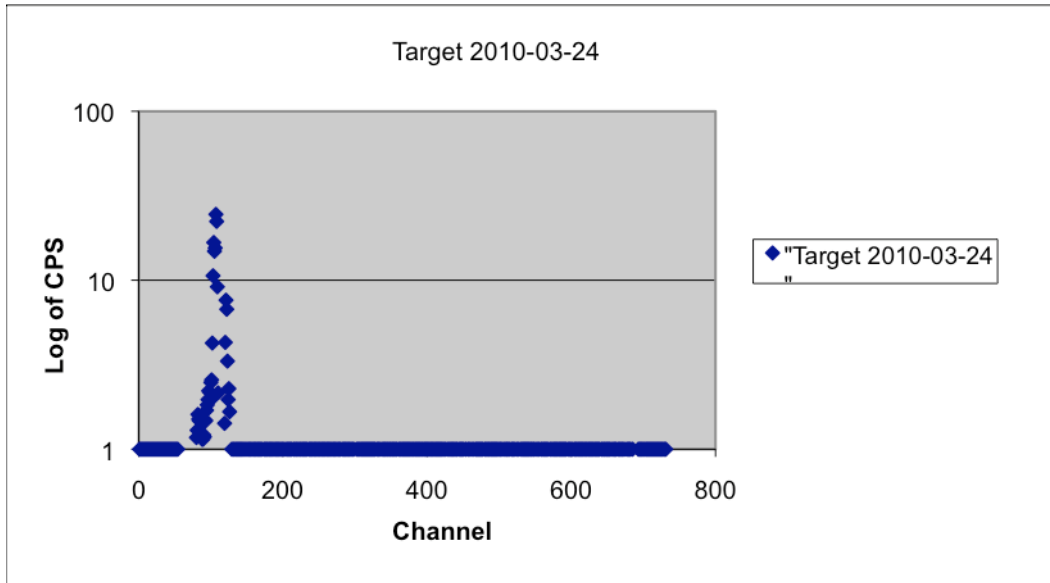
Plot 6: Spectrum from the HPGe detector of the ^{211}At target 2010-03-10.



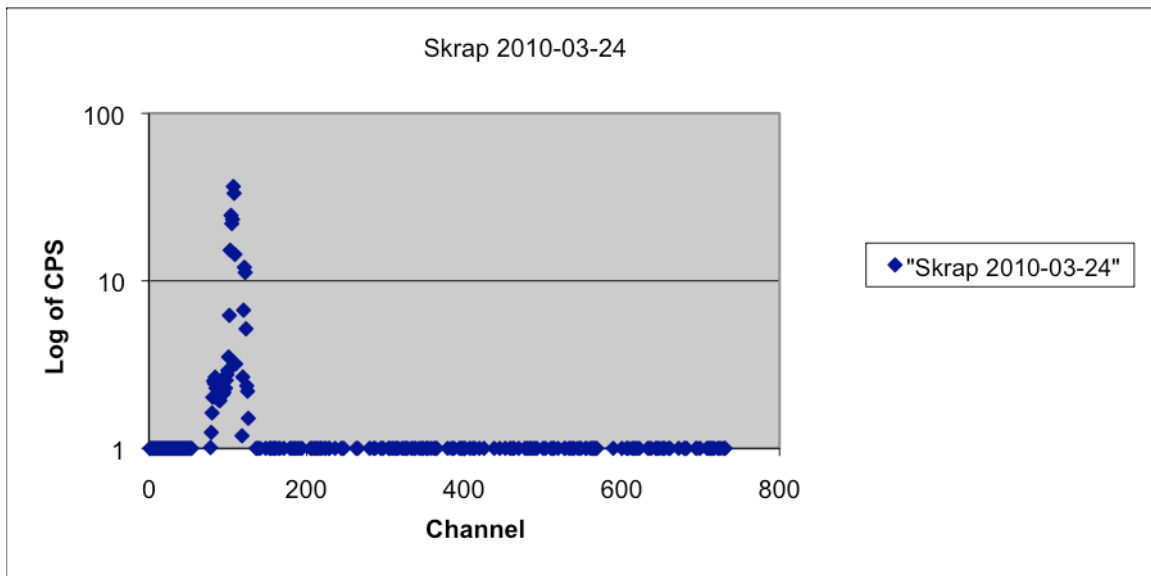
Plot 7: Spectrum from the HPGe detector of the ^{211}At scrapings 2010-03-10.



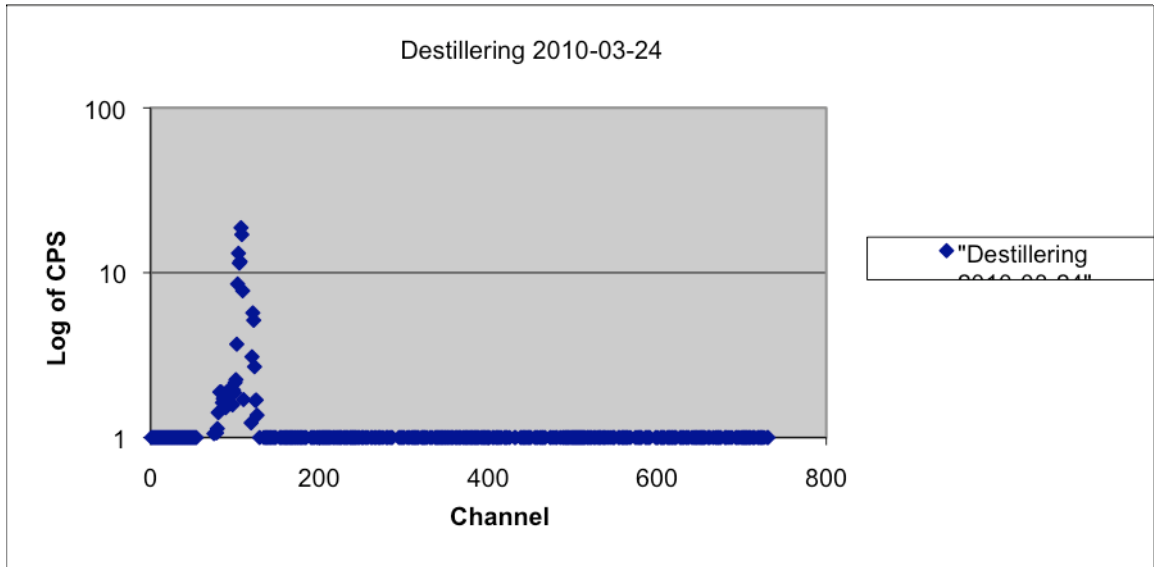
Plot 8: Spectrum of the HPGe detector of the distillation process 2010-03-10.



Plot 9: Spectrum of the HPGe detector of the target 2010-03-24.

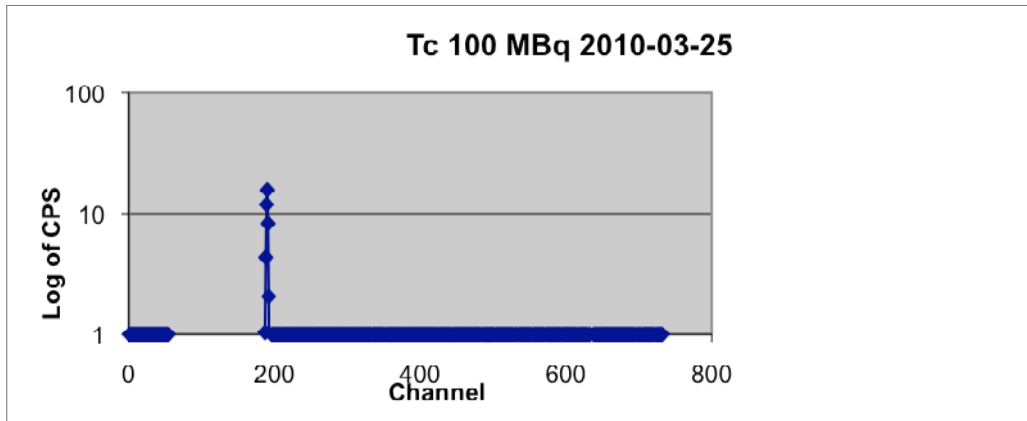


Plot 10: Spectrum of the HPGe of the ^{211}At scrapings 2010-03-24.



Plot 11: *Spectrum of the HPGe of the distillation process 2010-03-24.*

In Plot 12 below, the results from an HPGe measurement with technetium instead of astatine was conducted to ensure the origin of any found contamination, i.e. if a contamination wasn't registered in either on there is no contamination, if a contamination was registered in both of the measurements the origin probably originates from the laboratory and if a contamination was registered in the astatine spectrum the contamination most likely originates from the target activation.



Plot 12: Spectrum from the HPGe detector of a scintillation vial with a solution of PBS and 100 MBq ^{99m}Tc .

Table 1: The activity calibration factor calculations, types of measurements and the deviations from the mean value.

²¹¹ At	CPS	Activity (MBq)	MBq/CPS	(MBq/CPS)/Mean value	Type of measurement
1	2380	518	0.218	0.890	Target measurement
2	2804	536	0.191	0.782	Target measurement
3	2536	522	0.206	0.842	Target measurement
4	1928	513	0.266	1.088	Scrapings
5	3199	564	0.176	0.720	Target measurement
6	1720	582	0.338	1.383	Scrapings
7	1990	630	0.317	1.294	Scrapings
Mean value			0.245		

Table 1 (above) shows the activity calibration results. The table shows measurements from 7 different occasions. The values from the measurements fluctuates less if they are divided into subgroups shown in Table 2, below. The values are shown with mean values, deviation from the mean and also standard error of the mean (SEM). As mentioned in the Material and Methods part, a measurement of the scrapings in the IC was conducted only at one occasion. For the measurement of the backing after the scraping subtracted from the activity measurement of the target prior to the scraping, the resulting activity was 599 MBq (606 MBq- 7MBq) compared to the activity measurement of the scrapings which was 577 MBq.

Table 2: The activity calibration factors divided into groups depending on the type of measurement and the deviations from the mean value.

²¹¹At	Target measurements (activity from ionizing chamber) (MBq/CPS)	Target measurement (activity from ionizing)/Mean value	Measurement of scrapings (MBq/CPS)	Measurement of scrapings/Mean value
	0.218	1.100	0.266	0.840
	0.191	0.967	0.338	1.069
	0.206	1.041	0.317	1.031
	0.176	0.891		
Mean value	0.198		0.307	
SEM	0.009		0.021	

In Table 3 a series of measurements were conducted to simulate the geometry of the astatine experiments. All the geometries include pertechnetate in liquid form. The “target measurement” consists of undiluted pertechnetate in volumes around ~0.1mL, the “static measurement in a Teflon tube” is the volume from the previous “target measurement” only diluted to match the volume of the tube. The “diluted target to meet the geometry demands of the IC” is a pertechnetate volume of ~0.1mL, diluted with a volume of PBS such that the total volume of the solution amounts to 10mL. The IC is calibrated for solutions of this volume and the last measurements were conducted to ascertain that the difference in geometry wouldn’t matter.

Table 3: The activity calibration factor, types of measurements for ^{99m}Tc and the deviation from the mean value.

^{99m}Tc	CPS	Activity (MBq)	MBq/CPS	(MBq/CPS)/Mean value	Type of measurement
1	1573	85.1	0.054	0.909	Target measurement
2	1113	62.7	0.056	0.947	Static measurement in Teflon tube
3	2292	129.8	0.057	0.952	Target measurement
4	1060	59.4	0.056	0.942	Static measurement in Teflon tube
5	1398	95.7	0.068	1.151	Target measurement
6	81	5.23	0.065	1.085	Static measurement in Teflon tube
7	1277	96.5	0.076	1.270	Diluted target to meet the geometry demands of the IC
8	1951	109.2	0.056	0.941	Target measurement
9	97	5.55	0.057	0.962	Static measurement in Teflon tube
10	1985	109.1	0.055	0.924	Diluted target to meet the geometry demands of the IC
11	1512	82.6	0.055	0.918	Diluted target to meet the geometry demands of the IC
Mean value			0.059		

Table 4: The activity calibration factor for the ^{99m}Tc measurements divided into groups depending on the type of measurement.

^{99m}Tc	Target measurement (MBq/CPS)	Target measurement/Mean value	Static measurement in Teflon tube (MBq/CPS)	Static measurement in Teflon tube/Mean value	Diluted target to meet the geometry demands of the IC (MBq/CPS)	Diluted target to meet the geometry demands of the IC/Mean value
	0.054	0.920	0.056	0.962	0.076	1.224
	0.056	0.963	0.056	0.957	0.055	0.891
	0.068	1.164	0.065	1.103	0.055	0.885
	0.056	0.952	0.057	0.977		
Mean value	0.059		0.059		0.061	
SEM	0.003		0.002		0.007	

Table 5, shown below, show the test in y-led position. In the bottom row all the values are compared to the position in the Styrofoam cylinder, since the setup is calibrated to this position.

Table 5: The table shows a test in position. The position in the Styrofoam cylinder gives the maximum amount of counts because the system is set up in this fashion.

	2010-05-17 In Styrofoam cylinder CPS	2010-05-17 2 cm above fume hood CPS	2010-05-17 4 cm above fume hood CPS	2010-05-17 5 cm above fume hood CPS	2010-05-17 6 cm above fume hood CPS	2010-05-17 7 cm above fume hood CPS	2010-05-17 8.5 cm above fume hood CPS	2010-05-17 11.5 cm above fume hood CPS	2010-05-17 15 cm above fume hood CPS	2010-05-17 25 cm above fume hood CPS
65	1188	715	1056	1030	1049	1077	1037	955	889	626
71	1257	732	1057	1016	1019	1057	1006	980	869	602
59	1244	712	1061	1021	1022	1096	1048	989	905	646
55	1265	718	1015	980	1066	1102	1034	1007	938	597
72	1270	700	1056	982	1041	1037	1014	982	908	639
60	1165	724	1022	1035	1061	1102	1070	953	899	604
62	1198	701	1027	974	1072	1037	1015	979	870	592
65	1214	702	1039	1016	1067	1079	1091	1000	919	633
63.625	1225.125	713	1041.625	1006.75	1049.625	1073.375	1039.375	980.625	899.625	617.375

Compared to the level in the Styrofoam cylinder

1	0.58	0.85	0.82	0.86	0.88	0.85	0.80	0.73	0.50
---	------	------	------	------	------	------	------	------	------

In Table 6 the calibration factors from Table 2 is used to calculate a theoretical activity. This value is then compared (in Table 7) to the measured value of activity in the astatine eluated from the PEEK tube.

Table 6: The mean value of the plateau in the distillation plots were multiplied with the respective activity calibration factor from Table 2. At the bottom of the table the values from the IC measurement is shown.

	2010-03-10	2010-03-23	2010-04-07	2010-04-14	2010-04-21
211-At	<i>The mean value of the plateau in the distillation graph (CPS)</i>	<i>The mean value of the plateau in the distillation graph (CPS)</i>	<i>The mean value of the plateau in the distillation graph (CPS)</i>	<i>The mean value of the plateau in the distillation graph (CPS)</i>	<i>The mean value of the plateau in the distillation graph (CPS)</i>
	1330	1268	1614	1544	1977
<i>MBq calculated with the activity factor 0.198</i>	263	251	319	305	392
<i>MBq calculated with the activity factor 0.307</i>	408	389	496	474	607
<i>MBq measured in the IC</i>	301	298	328	446	502

Table 7: The values of the measured and calculated activity is compared to the activity measured in the lab with the IC.

211-At	<i>1-(MBq calculated with the activity factor 0.198/MBq from the notes taken at the measurement)</i>	<i>1-(MBq calculated with the activity factor 0.307/MBq from the notes taken at the measurement)</i>
3/10/10	0.126245847	0.355481728
3/23/10	0.157718121	0.305369128
4/7/10	0.027439024	0.512195122
4/14/10	0.316143498	0.062780269
4/21/10	0.219123506	0.209163347

In Table 8, the same calculations as in Table 7 was made but with the end point of the distillation curve instead of the mean value of the supposed plateau. In Table 9 the values from the calculations are compared to the measured ones.

Table 8: The table shows calculations of the theoretical value of the activity and the measured value from the IC. Instead of using the mean value of the plateau, the end-point value has been used.

	2010-03-10	2010-03-23	2010-04-07	2010-04-14	2010-04-21
211-At	<i>The end value of the plateau in the distillation graph (CPS)</i>	<i>The end value of the plateau in the distillation graph (CPS)</i>	<i>The end value of the plateau in the distillation graph (CPS)</i>	<i>The end value of the plateau in the distillation graph (CPS)</i>	<i>The end value of the plateau in the distillation graph (CPS)</i>
	1348	1306	1684	1610	1977
MBq calculated with the activityfactor 0.198	267	259	333	319	397
MBq calculated with the activityfactor 0.307	413	400	517	494	607
MBq from the notes taken at the measurement	301	298	328	446	502

Table 9: The table shows the theoretical value of the activity compared to the measured value.

211-At	1-(MBq calculated with the activity factor 0.198/MBq from the notes taken at the measurement)	1-(MBq calculated with the activity factor 0.307/MBq from the notes taken at the measurement)
3/10/10	0.112956811	0.372093023
3/23/10	0.130872483	0.342281879
4/7/10	-0.015243902	0.576219512
4/14/10	0.284753363	0.107623318
4/21/10	0.209163347	0.209163347

In Table 10 the values of the point of measure at 90 s (the time when the water jet is turned down) and compares it with the end point of the distillation plot.

Table 10: *The table show a comparison between a measuring point at 90 s (the time when the water jet is slowed down) and the end point of the distillation plots.*

	2010-03-10 Distillation	2010-03-23 Distillation	2010-04-07 Distillation	2010-04-14 Distillation	2010-04-21 Distillation
Point at 90 s	1254	1222	1664	1441	1796
End point	1348	1306	1684	1610	1977
1-(Point at 90s/Endpoint)	0.069732938	0.06431853	0.011876485	0.104968944	0.091552858

Discussion

The astatine x-ray peak cluster was, as mentioned above, cut a bit at the lower energies, but this should not be a problem because all the measurements were carried out this way. But if an absolute measurement should be wanted in the future, the energy window for the current project should be observed, so the window can be changed without the data from this project being lost.

The distillation-buildup graphs sometimes show an increase of CPS immediately after the under-pressure from the water flow is decreased and sometimes the graph does not change at all. That is, after the under-pressure, caused by the water jet pump, was decreased; by turning the water flow down, the distillation plot sometimes increases and sometimes not. It is difficult to explain the reason for this but it is likely that the phenomenon depends on the way that the pressure ratios are handled and the fact that much of the process is manually operated and therefore not carried out in an exact fashion. There are some indications in earlier results that the appearances of the increase in the CPS in the beginning of the build-up graphs might have something to do with the properties of the target scrapings. If the scrapings are finely separated, to more resemble a powder, the curve has a tendency to grow more rapidly and also the amount of activity drawn from the scrapings seems to be slightly higher. But these are just speculations based on observations along the way.

The activity calibrations tend to fluctuate more if all the results are viewed together compared to if they are divide into subgroups (see Tables 1-2). That is, if the ²¹¹At measurements are divided into groups of “Target measurements” and “Scraping measurements” the values of the measurements do not fluctuate as much. There seems to be a conversion factor belonging to each group. But in theory this factor should not be different for these two groups. The factor should simply be a ratio between

the amount of activity in the point of measurement and the CPS detected in the detector. As said before the quartz boat with the scrapings are placed on top of bunched paper, which is placed in the Styrofoam cylinder. The target is simply placed at the bottom of the cylinder. In Table 5 the sensitivity in positioning in the y-axis is shown. The detector is positioned so that the maximum CPS is received around the bottom of the cylinder. This position is somewhere around 6–8 cm above the fume hood. From Table 5 we can see that there is a dependency in positioning in the y-led, but the difference is not sufficient to solely be the explanation for the conversion factor divergence and the difference in the positioning in the y-led due to the bunched up paper does not exceed 6-7 cm.

To further try to explore this problem a range measurements in different experimental situations using the nuclide ^{99m}Tc in the form of pertechnetate was performed. The interesting part in the results is shown in Table X. For the ^{211}At measurements the geometry seems to play a larger part than for ^{99m}Tc . The fact that the tube simulation gets about the same conversion factor as the target measurements, in the case of the technetium, is an indicator that geometry is not a big source of error. It is more likely that the difference in calibration factor is due to scattering. When the astatine is measured in target form the activity is at the top layers of said target. The case with the scrapings is much more complex. When the scrapings are mechanically removed the entire layer of bismuth is removed, not just the layer with the astatine. Some of the flakes of un-activated bismuth are likely to cover the flakes with astatine. Since bismuth has a high Z value ($Z= 83$ and a mass attenuation coefficient of $\sim 1.85\text{-}2.55 \text{ cm}^2/\text{g}$) it is probable that this is the main source of error for these measurements.

One of the subprojects in this thesis was to investigate whether or not there could be any contamination in the target, due to activational products. The theory behind this project was based on fact that the activity in the target may be overestimated if it is contaminated with a nuclide that may not get distilled. A contamination may also be the cause to false results regarding the astatine activity if it to some extent gets distilled. This problem was investigated with

the help of the HPGe detector mentioned above. The results shown in Plots 6-11 indicate that no contamination worth mentioning seem to exist.

In Table 6 and 7 the mean values of the plateaus in the distillation graphs are used to calculate the theoretical values of the activity received from the process. These are then compared to the value measured with the IC in the lab. From the tables it is clear that the activity calibration is not complete. The values are simply not showing any tendencies. If one compares the results in Table 7 with the visual results in Plots 1-5, there is an indication that the plateau is not reached in all the cases, that there is still a flow of activity into the PEEK tube when the measurement ends. In the future it could be an idea to let the measurement continue until a plateau is reached. The comparisons in Tables 6-9 indicate that a sufficient plateau is not reached and that activity calibration at this stage is not possible or meaningful.

Conclusion

As mentioned above in the discussion the activity calibration is not complete. More measuring is needed to get statistically significant values. The current 4-5 measurements are simply not enough to base a correction factor on. And the measurements of the plateau should be prolonged until there actually is a stable plateau. The fact that the plateau is not entirely reached is also an indication that there is more activity in the scrapings to get. In Table 10 the results are fluctuating but the difference in the CPS are as high as 10%. But again more measurements are needed to actually see a trend, and a longer measuring time.

According to results in this project there were no contaminations from products from the activation process to be found but this does not mean that the possibility can be excluded. But this thesis indicates that if there is a contamination its contribution is insignificant.

In the method part of this thesis it was said that the energy window of the rate meter was set to include all energies. The next step is to set the window to the energy of the X-ray cluster of ^{211}At . By setting the window to this range of energy and do measurements on the target both prior to mechanically separating it from the backing and after.

References

Anderson H, Cederkrantz E, Bäck T, Divgi C, Elgqvist J, Himmelman J, Horvath G, Jacobsson L, Lindegren S, Palm S and Hultborn R. (2009) Intrapertoneal Alpha-particle Radioimmunotherapy of Ovarian Cancer Patients: Pharmacokinetics and Dosimetry of ^{211}At -MX35 F(ab')₂ – A Phase I Study (2009) *J Nucl Med* 50 : 1153-1160

Lindegren S, Frost S, Bäck T, Direct Procedure for the Production of ^{211}At -labeled Antibodies with an ϵ -Lysyl-3-(Trimethylstannyl)Benzamide Immunoconjugate, 2007.

Andersson H, Lindegren S, Bäck T, The Curative and Palliative Potential of the Monoclonal Antibody MOv18 Labeled with ^{211}At in Nude Mice with Intraperitoneally growing Ovarian Cancer Xenografts, 2000.

Acknowledgements

I'd like to begin by thanking my supervisor Sture Lindegren for bringing me into this project and giving me help and support through it. It has been hard but interesting. I would also like to thank Sofia Frost and Tom Bäck for making the early mornings fun, and for taking the time to answer all my questions. My gratitude also goes out to Jörgen Elgqvist, Nils Rudqvist and Lars Jacobsson for always having time for brainstorming and discussion. I also thank Daniela Marcocsan for taking the time to help me.

I'd like to thank my classmates, both in Lund and in Gothenburg for making these past years so great and at last Cristian for being such a calm and patient support.